

Bacterial cell division protein FtsZ assembles into protofilament sheets and minirings, structural homologs of tubulin polymers

HAROLD P. ERICKSON*[†], DIANNE W. TAYLOR*[‡], KENNETH A. TAYLOR*[‡], AND DAVID BRAMHILL[§]

*Department of Cell Biology, Duke University Medical School, Durham, NC 27710; and [§]Department of Enzymology, Merck Research Laboratories, Rahway, NJ 07065

Communicated by Robert L. Hill, Duke University Medical Center, Durham, NC, October 9, 1995

ABSTRACT The bacterial cell division protein FtsZ is a homolog of tubulin, but it has not been determined whether FtsZ polymers are structurally related to the microtubule lattice. In the present study, we have obtained high-resolution electron micrographs of two FtsZ polymers that show remarkable similarity to tubulin polymers. The first is a two-dimensional sheet of protofilaments with a lattice very similar to that of the microtubule wall. The second is a miniring, consisting of a single protofilament in a sharply curved, planar conformation. FtsZ minirings are very similar to tubulin rings that are formed upon disassembly of microtubules but are about half the diameter. This suggests that the curved conformation occurs at every FtsZ subunit, but in tubulin rings the conformation occurs at either β - or α -tubulin subunits but not both. We conclude that the functional polymer of FtsZ in bacterial cell division is a long thin sheet of protofilaments. There is sufficient FtsZ in *Escherichia coli* to form a protofilament that encircles the cell 20 times. The similarity of polymers formed by FtsZ and tubulin implies that the protofilament sheet is an ancient cytoskeletal system, originally functioning in bacterial cell division and later modified to make microtubules.

FtsZ is an abundant bacterial protein essential for cell division in all bacterial species investigated (1). Outside bacteria, FtsZ has recently been discovered in *Arabidopsis* as a nuclear-encoded gene that is transported into chloroplasts (2). A second *Arabidopsis* FtsZ (partial) sequence is in the dbEST data base (GenBank accession no. Z48464). FtsZ may form the cytoskeletal framework for cell division in all bacteria, as well as chloroplasts and mitochondria.

FtsZ has been identified as a homolog of tubulin on the basis of limited but convincing sequence similarity and its binding and hydrolysis of GTP (refs. 3–5; reviewed in ref. 6). Two laboratories have reported assembly of FtsZ into protofilaments and into larger rods or tubular polymers (7, 8). The subunit lattice of these polymers was not clearly resolved but appeared different from that of microtubules. Thus, the structural relation of FtsZ polymers to tubulin remained unclear.

The most important place to look for structural similarity is at the level of the subunit lattice because it is this lattice that is dictated by the repeating protein–protein contacts. The gross structure of the polymer is less important as an indicator of conserved structure. An open microtubule wall is shown in Fig. 1A, and a computer-reconstructed image of the subunit lattice is shown in Fig. 2A. The two-dimensional (2D) lattice consists of subunits, alternating α - and β -tubulin, in a parallel array of longitudinal protofilaments. Subunits are 4.0 nm apart along the protofilament, and the protofilaments are 5.1 nm apart laterally (9). If FtsZ polymers are structurally homologous to a microtubule, we should expect to see long, straight

protofilaments, which could associate further to make 2D sheets.

Mukherjee and Lutkenhaus (7) have already demonstrated assembly of purified FtsZ into protofilaments. These protofilaments were about 5 nm in diameter (after subtracting 1 nm for the shell of metal) and mostly straight or gently curved; the subunit spacing along the protofilaments was not resolved. Under these conditions, the protofilaments assembled from pure FtsZ did not assemble further into larger arrays. Larger polymers were eventually obtained by using a trick demonstrated many years ago with tubulin. Erickson and Voter (10) had found that assembly of MAP-free tubulin could be stimulated by a variety of polycations, including DEAE dextran. Mukherjee and Lutkenhaus (7) found that a mixture of DEAE dextran and FtsZ assembled into long, rod-shaped or tubular polymers. However, these polymers did not show the parallel arrangement of longitudinal protofilaments characteristic of the microtubule lattice.

In an independent study, Bramhill and Thompson (8) reported assembly of purified FtsZ into large polymers that could be pelleted in the ultracentrifuge. Their negatively stained specimens showed rods with an indication of a protofilament structure, but these also seemed quite different from the microtubule lattice. (We have now discovered that the large polymers reported by Bramhill and Thompson are obtained only at low pH. The FtsZ was originally in a Tris buffer at pH 7.5, but the addition of 6 mM GTP dropped the pH to 5.5–6. The present work and studies to be reported elsewhere demonstrate that protofilaments are assembled over the complete range, from pH 5.5 to 7.0. Subsequent assembly into large bundles of protofilaments is enhanced at lower pH.)

In addition to the 2D sheet of protofilaments, tubulin forms ring-shaped polymers with an outer diameter of 38–43 nm (11–13). Electron microscopy of microtubules in the process of assembly or disassembly identified these rings as single protofilaments in a sharply curved conformation (12, 13). When bonded to other subunits in the microtubule wall, the protofilament remains straight, but, when it peels away from the wall, it snaps into the curved conformation and forms rings. Recent cryoelectron microscopy of rapidly frozen microtubules shows a bouquet of curved protofilaments and rings at the end of disassembling microtubules (14). This suggests a possible role in microtubule depolymerization (15), but a convincing function for tubulin rings is still unknown. Without a definitive function for rings, it was easy to dismiss them as perhaps an unimportant structural accident. We did not expect to find similar ring polymers formed by FtsZ.

In the present study, we have used negative stain electron microscopy, optical diffraction, and computer reconstruction

Abbreviations: 2D, two dimensional; MAP, microtubule-associated protein.

[†]To whom reprint requests should be addressed at: Department of Cell Biology, 3011, Duke University Medical School, Durham, NC 27710.

[‡]Present address: Institute of Molecular Biophysics, Florida State University, Tallahassee, FL 32306-3015.

The publication costs of this article were defrayed in part by page charge payment. This article must therefore be hereby marked "advertisement" in accordance with 18 U.S.C. §1734 solely to indicate this fact.

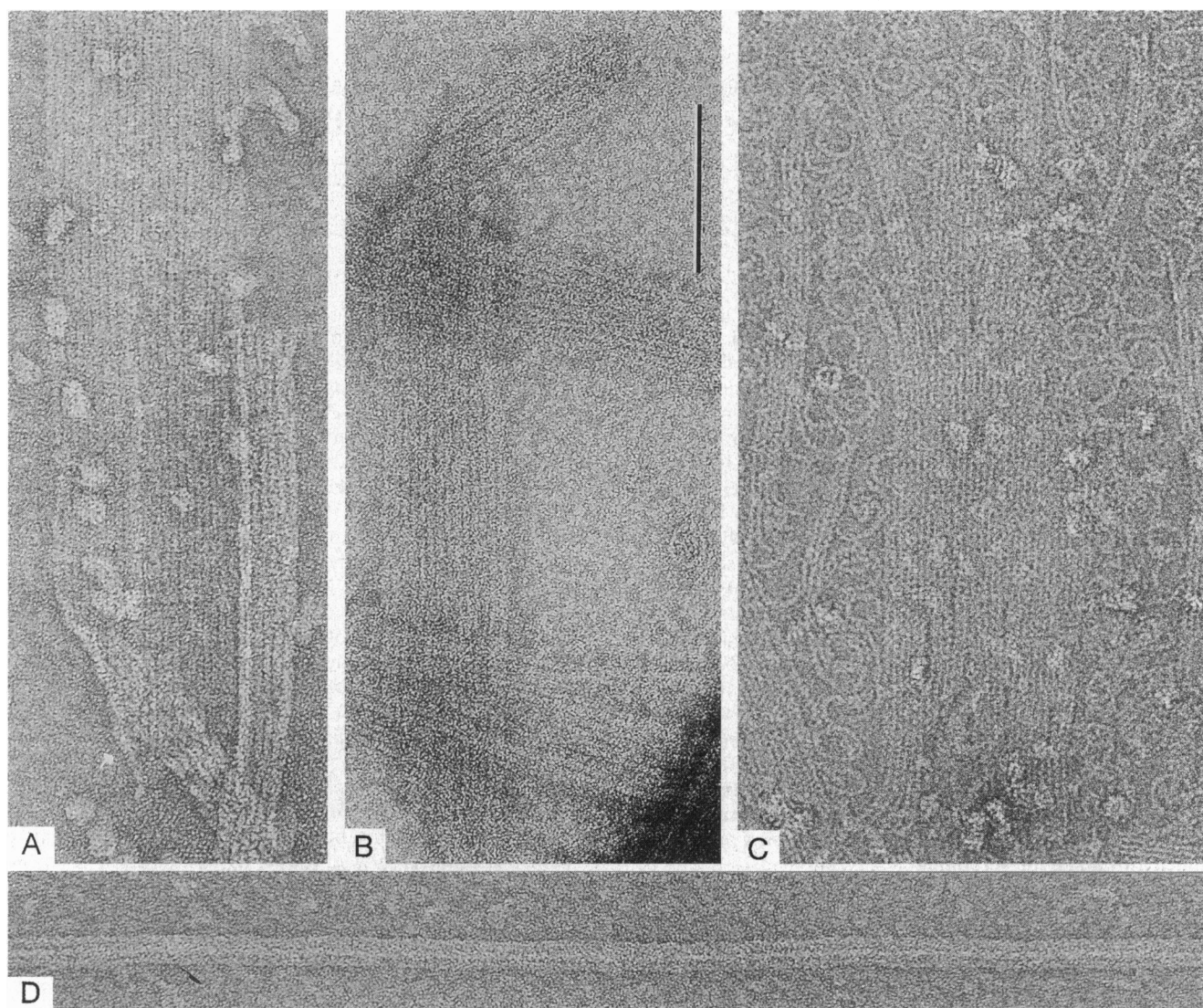


FIG. 1. Protofilament sheets formed by pig brain tubulin plus taxol (*A*) (Note the intact microtubule on the right edge of the large sheet of protofilaments and the one at the bottom continuous with the sheet.); FtsZ plus DEAE dextran (*B*) (Note three protofilament sheets crossing each other and the single miniring on the right.); FtsZ adsorbed to a monolayer of cationic lipid (*C*) (Note the large sheet of protofilaments in the middle and several smaller ones; there are several examples of protofilaments peeling off the edges of sheets and forming minirings; there are also many intact minirings.); and purified FtsZ polymerized for 60 min at 37°C at pH 7 with GTP in the absence of any stabilizing polycations (*D*). (Bar in *B* = 100 nm.)

to obtain higher resolution images of the lattice of FtsZ polymers.

MATERIALS AND METHODS

Phosphocellulose-purified tubulin was prepared from pig brain and polymerized at 3 mg/ml with 20 μ M taxol in a Pipes/Mg²⁺/EGTA/GTP buffer, pH 7.4 (16). After 40 min at 37°C the microtubules were diluted 1/10, and negatively stained samples were prepared. FtsZ was purified from a pET expression system as described (8) and stored frozen as a stock at 10 mg/ml.

For assembly with DEAE dextran, FtsZ was diluted to 0.5 mg/ml in 100 mM Mes/50 mM potassium acetate/2 mM EGTA/5 mM magnesium acetate/2 mM GTP (pH 6.5). DEAE dextran (Sigma) was added to a concentration of 0.1 mg/ml. After 30 min on ice, the sample was warmed to 37°C, and negatively stained specimens were prepared 5 min later.

For assembly on the lipid monolayer, the buffer contained Mops, pH 7.0, instead of Mes, and in some experiments 2 mM GDP was substituted for GTP. A total of 30 μ l of buffer at

room temperature was overlaid with 0.75 μ g of a 70:30 mixture of dilaurylphosphatidylcholine to didodecyldimethylammonium in chloroform (17, 18). FtsZ was injected into the buffer at room temperature to give a concentration of 0.3 mg/ml. The sample was incubated at room temperature for 60 min and then moved to 2°C for 10 min, and the lipid monolayer with adsorbed protein polymers was lifted on a holey carbon film and negatively stained as described (17, 18). Attempts to lift the monolayer at room temperature were not successful. All samples were negatively stained with two or three drops of 2% aqueous uranyl acetate.

Electron micrographs were taken at a magnification of $\times 50,000$. Magnification was calibrated by photographing negatively stained tropomyosin paracrystals and assuming a period of 38.8 nm. All micrographs used for measurements were collected over a period of several days, interspersed with tropomyosin calibration. The calibration photographs varied by only $\pm 1\%$.

RESULTS AND DISCUSSION

FtsZ Forms 2D Sheets of Protofilaments Similar to the Microtubule Wall. We have confirmed that assembly of FtsZ

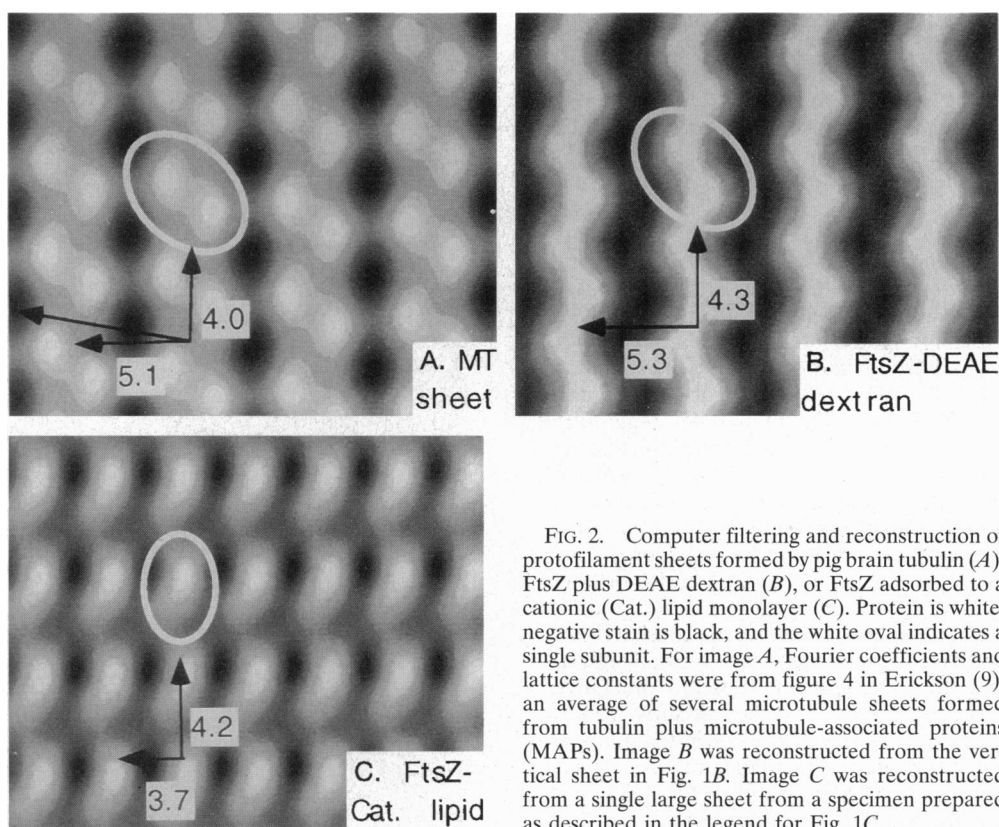


FIG. 2. Computer filtering and reconstruction of protofilament sheets formed by pig brain tubulin (A), FtsZ plus DEAE dextran (B), or FtsZ adsorbed to a cationic (Cat.) lipid monolayer (C). Protein is white, negative stain is black, and the white oval indicates a single subunit. For image A, Fourier coefficients and lattice constants were from figure 4 in Erickson (9), an average of several microtubule sheets formed from tubulin plus microtubule-associated proteins (MAPs). Image B was reconstructed from the vertical sheet in Fig. 1B. Image C was reconstructed from a single large sheet from a specimen prepared as described in the legend for Fig. 1C.

with DEAE dextran at pH 7.2 produces tubular polymers (7). In some images, protofilaments are resolved spiraling in a shallow helix (see figure 2 in ref. 6), similar to the outer wall of the double-wall microtubules formed by tubulin plus DEAE dextran (10). These spiral tubules are not physiologically important for tubulin and are probably not for FtsZ.

In these specimens prepared at pH 7.2, we occasionally observed long, straight protofilaments associated in pairs or in larger 2D sheets. These 2D sheets of protofilaments were much more prominent in a pH 6.5 buffer. Many examples could be found with 10–15 or more protofilaments in a highly ordered, parallel array. A micrograph of these FtsZ–DEAE dextran sheets is shown in Fig. 1B. There is a remarkable similarity to the eukaryotic microtubule wall in Fig. 1A.

In an effort to produce more highly ordered 2D arrays, we next turned to a technique of 2D crystal formation on positively charged lipid monolayers, which had produced very large and highly ordered arrays of actin (17, 18). We were encouraged by the thought that the polycationic lipid monolayer might stabilize FtsZ polymers similar to the stabilization by polycationic DEAE dextran in solution. These samples were incubated for 60 min at room temperature followed by 5–10 min at 2°C, so there was the possibility for assembly followed by disassembly. Negatively stained specimens (Fig. 1) showed three polymer forms that are structurally related to tubulin polymers: (i) large 2D sheets of parallel protofilaments; (ii) long, straight protofilaments that are single and separate; and (iii) curved protofilaments and minirings. Assembly at either pH 6.0 or pH 7.0 produced the same structures.

We have tested several buffer conditions for assembly of FtsZ in the absence of polycation stabilizing agents. Fig. 1D shows a long, narrow protofilament sheet or bundle obtained reproducibly at pH 7. These sheets are 20 nm wide, with 4 or 5 protofilaments, and quite long. The extra (white) density down the middle suggests possibly another protofilament added on top of a simple sheet. The important conclusion is that single protofilaments (not shown) and protofilament

sheets can be assembled from FtsZ in the absence of stabilizing agents.

Optical Diffraction and Computer Image Reconstruction.

Images were selected for lattice analysis whose diffraction patterns showed a clear equatorial spot, giving the spacing between protofilaments, and one or more spots on the first layer line, giving the spacing of subunits along the protofilaments. These lattice parameters are summarized in Table 1.

The longitudinal subunit spacing along the microtubule protofilaments was measured in the present study to be 4.06 nm, essentially the same as the values of 4.0 nm and 4.05 nm reported in previous studies for the GDP-microtubule (9, 19, 20). The subunit spacing along the FtsZ protofilaments was 4.2–4.3 nm in the two types of sheets, slightly larger than the GDP-tubulin spacing but very close to that of GTP-tubulin (20). The lateral spacing between protofilaments in the microtubule wall was 5.3 nm in the present study, slightly larger than the 5.1 nm measured previously for microtubule sheets assembled with MAPs (9); possibly the taxol stabilization or the absence of MAPs increased the protofilament spacing in the present specimens. The protofilament spacing for the DEAE dextran FtsZ sheets was also 5.3 nm.

Table 1. Lattice dimensions measured from optical diffraction patterns of taxol-stabilized microtubule sheets and FtsZ sheets

| Structure | Subunit spacing along protofilament, nm | Spacing between protofilaments, nm |
|----------------------------------|---|------------------------------------|
| Microtubule wall (n = 6) | 4.06 ± 0.06 | 5.28 ± 0.13 |
| FtsZ plus DEAE dextran (n = 13) | 4.33 ± 0.05 | 5.31 ± 0.30 |
| FtsZ plus cationic lipid (n = 9) | 4.19 ± 0.22 | 3.66 ± 0.26 |

Average and standard deviation are given for the indicated number (n) of images measured.

The FtsZ sheets on lipid monolayers showed the same 4.2-nm longitudinal spacing, but the lateral spacing between protofilaments was only 3.7 nm. The simplest explanation for the shorter lateral spacing is to propose that the FtsZ protofilaments have an oblong profile in cross section and are rotated about a longitudinal axis in the two types of sheets. Thus, in the DEAE dextran-stabilized sheets, protofilaments may be laterally bonded across the widest (5.3 nm) profile, while in the lipid monolayer-stabilized sheets they are rotated perhaps 90° and are bonded across the narrow (3.7 nm) profile.

Fourier computer reconstruction was used to filter nonperiodic noise and produce an averaged image of each of the three lattices (Fig. 2). As already noted, the lattice spacings of the DEAE dextran-stabilized FtsZ sheet are very similar to those of the microtubule wall. The subunits also appear very similar, being elongated and tilted at about a 45° angle to the protofilament. The one substantial difference is that the tubulin lattice is slightly skewed, such that subunits form a 10° angle perpendicular to the protofilaments. This angle produces a three-start helix in the intact microtubule. The FtsZ lattice does not have this skew and appears to be orthogonal.

The FtsZ–lipid monolayer lattice (Fig. 2C) is also orthogonal, but the subunits show a very different structure in projection. The different subunit structures are consistent with the hypothesis that these protofilaments are rotated substantially around a longitudinal axis from those in the DEAE dextran-stabilized sheets. In Fig. 2C, the subunits have an obvious polarity, and one can see that all protofilaments are pointing in the same direction. In these lipid-stabilized sheets, one can designate a plus and a minus end.

FtsZ Forms Minirings Similar to Tubulin Rings. In addition to straight protofilaments, ring-shaped polymers are very prominent in specimens of FtsZ adsorbed to the lipid monolayer, both in GTP (Fig. 1C) and GDP (Fig. 3). Their remarkable similarity to tubulin rings adds a new level to the structural homology of FtsZ and tubulin. We propose to call these “FtsZ minirings,” to avoid confusion with the terminology “FtsZ ring” that is already used to describe the accumulation of FtsZ around the bacterial membrane at the septation furrow. The minirings can be identified as protofilaments in a sharply curved conformation: there are several clear examples in Figs. 1C and 3, where protofilaments can be followed continuously from the 2D array to the curved conformation. This is very similar to the structure of rings attached to assembling or disassembling microtubule walls (12, 13).

We measured the outside diameters of the roundest minirings from several specimens. Two specimens assembled with GTP gave average diameters of 25.2 nm ($n = 24$) and 23.9 nm ($n = 32$). A specimen assembled with GDP (as in Fig. 3) gave an average diameter of 23.0 nm ($n = 28$). In all cases, the standard deviation was 1.6–1.9 nm, which reflected a substantial variation in the size of the minirings rather than measurement error. Minirings of smaller and larger diameter can be found in Fig. 3.

The 24-nm average diameter of FtsZ minirings is a bit more than half the 38- to 43-nm diameter of tubulin rings (11, 14). This may offer an important insight into the nature of the curved conformation in tubulin rings. The tubulin protofilament is alternating α and β subunits, while the FtsZ filament is made from a single type of subunit. It is reasonable to assume that in the FtsZ miniring all subunits are in the identical curved conformation. Does the tubulin ring involve curvature at both α and β subunits or only one? If the curved conformation occurs only at the β -tubulin subunit, with the α subunit remaining in the straight conformation, the tubulin rings should have approximately twice the diameter of FtsZ minirings. We conclude that the curved conformation of tubulin involves only one of the two subunits.

The curved conformation is found almost exclusively at the end of the protofilament and is usually continuous over a



FIG. 3. Protofilaments, small sheets, and minirings formed by FtsZ in GDP and adsorbed to the polycationic lipid monolayer. This specimen was prepared as described in the legend for Fig. 1C, except that GDP was substituted for GTP in the assembly buffer. The arrows indicate protofilaments that have separated from a sheet, remaining straight for some length, and then changing abruptly to the curved conformation. (Bar = 100 μm .)

length up to that needed to form a complete miniring (see arrows in Fig. 3). This implies that the transition to the curved conformation is initiated at the end and propagated, perhaps slowly, to successive subunits. When the curved segment is long enough to form a complete miniring, it probably breaks off and seals. We have noted on many specimens that the curved conformation is found at both ends of a protofilament sheet, indicating that it can occur at both the plus and minus ends of the protofilament, as it does with tubulin rings (14).

Tubulin rings exist transiently during microtubule depolymerization (14) and may play a role in the depolymerization process. The continuous coiling of protofilaments as the microtubule depolymerizes could also generate force, and might be involved in depolymerization-coupled translocation of microtubule bound particles (21). Whatever the role of these rings, it seems to be conserved from FtsZ to tubulin.

The Role of GTP and GDP. Microtubule assembly is favored by GTP and inhibited by GDP under most conditions. Normally the GTP is hydrolyzed, such that the microtubule wall (except for the GTP cap) contains only GDP-tubulin subunits. However, microtubules with a virtually identical lattice can be assembled from nonhydrolyzable GTP analogs (20). FtsZ protofilament sheets stabilized by polycations can be assembled in either GTP or GDP. On the lipid monolayer, the sheets formed in GDP (Fig. 3) are narrow, only 2–4 protofilaments, but appear to have the same substructure as those formed in

GTP. We have also found that FtsZ plus DEAE dextran assembled into large protofilament sheets in GDP (data not shown), consistent with the assembly of spiral tubules, which also occurs in GTP and GDP (7). We have not yet determined the nucleotide content of FtsZ sheets stabilized by DEAE dextran.

Tubulin rings can be assembled in the presence of either GTP or GDP (11) but are favored in GDP (15). It is possible that rings formed in GTP have hydrolyzed the GTP and carry GDP. FtsZ minirings stabilized by the cationic lipid monolayer were also assembled in either GTP or GDP, and they seemed to be favored in GDP (Fig. 3). We have not yet been able to obtain a fraction of FtsZ rings in solution that would permit nucleotide analysis.

Speculation on the Physiologically Important FtsZ Polymer and the Evolution of Microtubules. We conclude that the functional FtsZ polymer *in vivo* must be some form of protofilament sheet, probably close to the long, narrow sheets or bundles observed at pH 7 (Fig. 1D). The geometry of a protein subunit that can assemble into a protofilament sheet is so complex and precise that this assembly could not exist *in vitro* unless it were constantly selected for and, hence, functionally important *in vivo*. To form a straight protofilament, longitudinal bonding interfaces must be exactly 180° apart on the subunit. To produce a flat sheet of protofilaments, lateral interfaces must also be 180° apart. Because all subunits make lateral bonds in the same plane, rotation of subunits about the protofilament axis must be precisely 0°. This precise geometry would not be preserved in evolution unless it were functionally important *in vivo*. The function of this geometry is clear for tubulin: it is essential to form the microtubule wall. Until now we have had little idea of what kind of polymers FtsZ formed *in vivo*, but we can now conclude that they must be based on the protofilament sheet. Still unknown are the length and width of the sheets *in vivo*, whether they stack in the third dimension, and what associated molecules might be involved.

The cytoskeletal role of FtsZ is also suggested by its abundance: 5,000–20,000 molecules of FtsZ in each *Escherichia coli* cell (22, 23). This gives a concentration of 1–3 mg/ml, similar to the concentration of tubulin in eukaryotic cells. A total of 10,000 molecules of FtsZ could make a single protofilament 40 μm long, enough to encircle a 0.6-μm diameter bacterium 20 times. If the actual FtsZ polymers are sheets of 2–4 protofilaments, there would still be enough for several overlapping sheets to encircle the cell. These could be anchored to the membrane at one end (perhaps a nucleation site) and perhaps bridged by motor proteins to form a contractile ring. One should also consider the possibility that forces generated in the transition from the straight protofilament to the miniring could be harnessed to achieve a contraction—i.e., that the protofilament itself is the motor driving contraction.

A scenario for the evolution of the FtsZ/tubulin cytoskeleton should postulate FtsZ as the primordial protein, since it is found in all bacteria examined. The protofilament sheet probably arose early in the evolution of cellular life forms and

was adopted as the cytoskeletal framework for a contractile ring that made cell division possible. This role has apparently been conserved in all bacterial species, as well as in chloroplasts and, perhaps, mitochondria, which arose as bacterial endosymbionts. Curiously, eukaryotic cells have replaced the FtsZ system with the actin-based cytoskeletal ring and use microtubules for very different functions.

Where did microtubules arise? Perhaps in a bacterium following a gene duplication that produced a redundant FtsZ. This second FtsZ, retaining the ability to form protofilament sheets, could gradually acquire mutations in the lateral bonds that would change it from a flat sheet to a curved one, and give it a helical pitch. Once the curvature and helical pitch hit angles that permitted closure to a cylinder, the mechanical rigidity of this new structure must have provided enormous new opportunities for developing the cytoskeleton.

This work was supported by National Institutes of Health Research Grants R37-CA47056 to H.P.E. and R01-AR42872 to K.A.T.

1. Lutkenhaus, J. (1993) *Mol. Microbiol.* **9**, 403–409.
2. Osteryoung, K. W. & Vierling, E. (1995) *Nature (London)* **376**, 473–474.
3. RayChaudhuri, D. & Park, J. T. (1992) *Nature (London)* **359**, 251–254.
4. de Boer, P., Crossley, R. & Rothfield, L. (1992) *Nature (London)* **359**, 254–256.
5. Mukherjee, A., Dai, K. & Lutkenhaus, J. (1993) *Proc. Natl. Acad. Sci. USA* **90**, 1053–1057.
6. Erickson, H. P. (1995) *Cell* **80**, 367–370.
7. Mukherjee, A. & Lutkenhaus, J. (1994) *J. Bacteriol.* **176**, 2754–2758.
8. Bramhill, D. & Thompson, C. M. (1994) *Proc. Natl. Acad. Sci. USA* **91**, 5813–5817.
9. Erickson, H. P. (1974) *J. Cell Biol.* **60**, 153–167.
10. Erickson, H. P. & Voter, W. A. (1976) *Proc. Natl. Acad. Sci. USA* **73**, 2813–2817.
11. Voter, W. A. & Erickson, H. P. (1979) *J. Supramol. Struct.* **10**, 419–431.
12. Erickson, H. P. (1974) *J. Supramol. Struct.* **2**, 393–411.
13. Kirschner, M. W., Williams, R. C., Weingarten, M. & Gerhart, J. C. (1974) *Proc. Natl. Acad. Sci. USA* **71**, 1159–1163.
14. Mandelkow, E.-M., Mandelkow, E. & Milligan, R. A. (1991) *J. Cell Biol.* **114**, 977–991.
15. Melki, R., Carlier, M.-F., Pantaloni, D. & Timasheff, S. N. (1989) *Biochemistry* **28**, 9143–9152.
16. McIlvain, J. M., Jr., Burkhardt, J. K., Hamm-Alvarez, S., Argon, Y. & Sheetz, M. P. (1994) *J. Biol. Chem.* **269**, 19176–19182.
17. Taylor, K. A. & Taylor, D. W. (1992) *J. Struct. Biol.* **108**, 140–147.
18. Taylor, K. A. & Taylor, D. W. (1994) *Biophys. J.* **67**, 1976–1983.
19. Wolf, S. G., Mosser, G. & Downing, K. H. (1993) *J. Struct. Biol.* **111**, 190–199.
20. Hyman, A. A., Chrétien, D., Arnal, I. & Wade, R. H. (1995) *J. Cell Biol.* **128**, 117–125.
21. Lombillo, V. A., Stewart, R. J. & McIntosh, J. R. (1995) *Nature (London)* **373**, 161–164.
22. Pla, J., Sanchez, M., Palacios, P., Vicente, M. & Aldea, M. (1991) *Mol. Microbiol.* **5**, 1681–1686.
23. Dai, K. & Lutkenhaus, J. (1992) *J. Bacteriol.* **174**, 6145–6151.